

## Signal-to-Noise Eigenmode Analysis of the Two-Year COBE Maps

J. Richard Bond

*Canadian Institute for Theoretical Astrophysics, University of Toronto, Toronto, Ontario, Canada M5S 1A7*  
(Received 15 July 1994)

To test best a theory of cosmic microwave background fluctuations, anisotropy maps [here the two-year Cosmic Background Explorer differential microwave radiometer (DMR) 53, 90, 31 GHz  $a$  and  $b$  and the Far-Infrared Survey (FIRS) 170 GHz maps] are expanded in a complete basis of linear combinations of pixel amplitudes—statistically independent for both the noise and the signal. Bayesian analysis of a 2-parameter inflation-inspired theory shows the overall band-power and spectral tilt index  $\nu_{\Delta T} + 1$  for all maps agree within  $1\sigma$ ,  $\{(1.1 \pm 0.1) \times 10^{-5}\}^2$  and  $1.27 \pm 0.33$  (compatible with inflation values,  $\sim 0.8-1.2$ ); and  $S/N$  filtering of the DMR maps reveals the same large-scale structural features.

PACS numbers: 98.70.Vc, 98.80.Cq, 98.80.Es

The importance of the large-angle Cosmic Background Explorer (COBE) differential microwave radiometer (DMR) [1,2] and the Far-Infrared survey (FIRS) (a balloon-borne cosmic background radiation experiment) [3] detections for testing theories of cosmic structure formation can hardly be overstated. For theories in which the multipole components of the radiation pattern  $a_{\ell m}$  are Gaussian distributed and statistically independent, as in inflation-based models or via the central limit theorem, we only need to determine the power spectrum,  $C_\ell \equiv \ell(\ell + 1) \langle |a_{\ell m}|^2 \rangle / (2\pi)$ . A phenomenology characterized by just two parameters, a broad-band power  $\langle C_\ell \rangle_{\text{DMR}}$  and a broad-band tilt  $\nu_{\Delta T}$ , is an excellent approximation for a large class of models:

$$C_\ell = \langle C_\ell \rangle_{\bar{W}} \frac{\mathcal{U}_\ell I[\bar{W}_\ell]}{I[\bar{W}_\ell \mathcal{U}_\ell]}, \quad \mathcal{U}_\ell \equiv \frac{\Gamma(\ell + \nu_{\Delta T}/2) \Gamma(\ell + 2)}{\Gamma(\ell) \Gamma(\ell + 2 - \nu_{\Delta T}/2)},$$

$$\langle C_\ell \rangle_{\bar{W}} \equiv \frac{I[C_\ell \bar{W}_\ell]}{I[\bar{W}_\ell]}, \quad I[f_\ell] \equiv \sum_e \frac{(\ell + \frac{1}{2})}{\ell(\ell + 1)} f_\ell,$$

where  $I[f_\ell]$  defines the “logarithmic integral” of a function  $f_\ell$ . For the DMR and FIRS maps, the broad-band filter  $\bar{W}_\ell$  encodes beam smearing and effects from pixelization; for other experiments it also encodes switching information. The virtue of the band power [4–6]  $\langle C_\ell \rangle_{\bar{W}}$  is that it is insensitive to the specific shape of  $C_\ell$ , whereas the often used [1] “ $Q_{\text{rms},PS}$ ” varies considerably:

$$\frac{Q_{\text{rms},PS}}{17.6 \mu\text{K}} \approx \frac{\langle C_\ell \rangle_{\bar{W}}^{1/2}}{10^{-5}} e^{-\alpha \nu_{\Delta T} (1 + 0.3 \nu_{\Delta T})},$$

$\alpha = 0.37$  for DMR, and  $\alpha = 0.55$  for FIRS. The broad-band tilt  $\nu_{\Delta T}$  measures deviation from scale invariance in  $\Delta T$ ,  $\mathcal{U}_\ell = (\ell + \frac{1}{2})^{\nu_{\Delta T}} [1 + \mathcal{O}((\ell + \frac{1}{2})^{-2})]$ . It is usual to use  $n_s = \nu_{\Delta T} + 1$  to characterize the slope [1] because for pure scalar metric fluctuations in a cold dark matter universe with almost no baryons  $n_s$  is the primordial (e.g., postinflation) index [7]. However, the standard 5% baryon content gives  $\nu_{\Delta T} = 0.15$  for an initially untilted primordial spectrum [5,8]; and primordial tilts, usually negative, can arise from gravitational wave as well as

density fluctuation modes, but with  $n_s > 0.7$  required to get the observed cluster abundance (e.g., [6,8]).

The observations  $(\Delta T/T)_p$  from the  $p$ th pixel of an  $N_{\text{pix}}$  cosmic microwave background anisotropy experiment is given to us in terms of an average value  $\langle \Delta T/T \rangle_p$  and a correlation matrix  $C_{Dpp'}$ , with possibly off-diagonal components as well as the diagonal  $\sigma_{Dp}^2$ . The theory we are testing is characterized by a correlation matrix  $C_{Tpp'}$  (here  $= I[C_\ell \bar{W}_\ell P_\ell(\cos \theta_{pp'})]$ , where  $\theta_{pp'}$  is the angle between pixels  $p$  and  $p'$ ). If signals are not Gaussian distributed, higher order correlation tensors are required, and such theories can only be well analyzed by simulation.

For this exploration of the DMR maps, I used one lower resolution scale than the original maps,  $5.2^\circ$  compared to  $2.6^\circ$ ; a Galactic latitude cut  $|b| > 25^\circ$  (leaving 928 pixels); dipole and average subtractions were done after cuts, but before resolution lowering; the (non-Gaussian) revision of the DMR beam [9], with corrections for digitization and pixelization; a correction linear in the off-diagonal  $C_D$  components to test sensitivity to residual correlation because COBE actually measures a  $\Delta T$  between pixels  $60^\circ$  apart [10]. For the 168 GHz FIRS map,  $2.6^\circ$  rather than  $1.3^\circ$  pixels were used (but I checked that the two give the same answer), leaving 1070 pixels; a  $3.9^\circ$  beam was used, which includes pixelization corrections.

A full Bayesian analysis of maps requires frequent inversion and determinant evaluations of  $N_{\text{pix}} \times N_{\text{pix}}$  correlation matrices, the sum of all  $C_{Tpp'}$  in the theoretical modeling plus the pixel-pixel observational error matrix  $C_{Dpp'}$ . To facilitate this, I expand the pixel values  $(\Delta T/T)_p$  into a basis of “signal-to-noise” eigenmodes for the maps in which the transformed noise and transformed (wanted) theoretical signal we are testing for do not have mode-mode correlations, i.e., are orthogonal. This can always be done, no matter what the experiment [4]. Complications are associated with the removal of averages, dipoles, etc., and the existence of secondary signals in the data, both of which do couple the modes. A model for the various contributions that make up the

observed data is then

$$\begin{aligned}\xi_k &= \sum_{p=1}^{N_{\text{pix}}} (RC_D^{-1/2})_{kp} (\Delta T/T)_p \\ &= s_k + (1+r)n_k + c_k + \text{res}_k, \quad k = 1, \dots, N_{\text{pix}}, \\ \langle s_k s_{k'} \rangle &= \mathcal{E}_{TR,k} \delta_{kk'} = (RC_D^{-1/2} C_T C_D^{-1/2} R^\dagger)_{kk'}, \\ \langle n_k n_{k'} \rangle &= \delta_{kk'}, \quad \langle \text{res}_k \text{res}_{k'} \rangle = \mathcal{R}_{kk'}, \quad \langle c_k c_{k'} \rangle = \mathcal{K}_{kk'}, \\ (\mathcal{E}_{\text{tot}R})_{kk'} &\equiv \mathcal{E}_{TR,k} + (1+r)^2 \delta_{kk'} + \mathcal{R}_{kk'} + \mathcal{K}_{kk'},\end{aligned}$$

where  $R$  is a rotation matrix. The modes are sorted in order of decreasing  $S/N$  eigenvalues,  $\mathcal{E}_{TR,k}$ , so low  $k$  modes probe the theory in question best. With uniform weighting and all-sky coverage, the  $S/N$  modes are just the independent  $\text{Re}(a_{\ell m})$  and  $\text{Im}(a_{\ell m})$ , with the lowest  $\ell$  having the highest  $\mathcal{E}_{TR,k}$ , hence  $k \sim (\ell + 1)^2$ . With inhomogeneous pixel coverage, Galactic cuts, dipole subtractions, etc., they are more complex.

This expansion is a complete (unfiltered) representation of the map. The sum of  $\xi_k^2$  over bands in  $S/N$  space defines a  $S/N$  power spectrum which gives a valuable picture of the data; an example is shown in Fig. 1. The maps can have an arbitrary average, dipole, and possibly quadrupole (because the Galactic contribution may contaminate the signal's quadrupole). This is modeled by

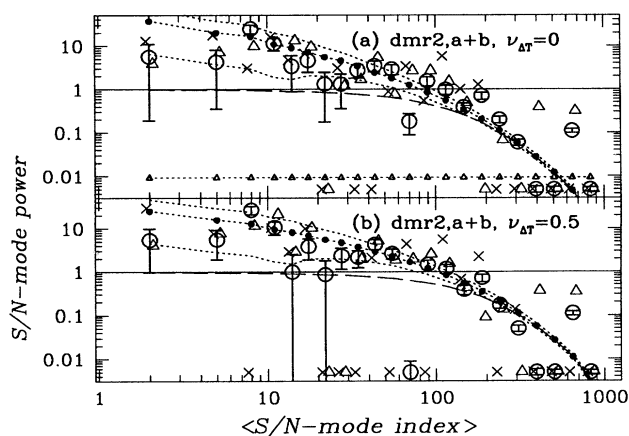


FIG. 1. The  $(S/N)$  band power (mean of  $\xi_k^2 - 1$  over a band in  $k$ ) for the DMR two-year  $53a + b$  maps, using the (a)  $\nu_{\Delta T} = 0$  and (b)  $\nu_{\Delta T} = 0.5$  modes. The observational error bars [smaller than the (open circle) points for  $k > 30$ ] include a large scale power correction. The  $<0.01$  values at high  $k$  are actually slightly negative. The small solid points joined by the central dotted curve give band averages of  $\mathcal{E}_{TR,k}$ , with the upper and lower dotted curves giving theoretical variances for this binning; all three scale with  $\langle C_\ell \rangle_{\text{DMR}}$ , thus can be raised or lowered to best fit the data. The horizontal line of solid triangles shows the most likely residual noise [tiny for (a), off-scale for (b)]. The Wiener filter is the long-dashed curve. The  $90a + b$  (open triangle) and  $31a + b$  ( $\times$ ) data points shown are uniformly scaled until their  $\mathcal{E}_{TR,k}$  agrees with  $53a + b$  (which they do); thus, given the larger error bars, the agreement in power among maps is reasonably good.

$c_k$ , with 4 or 9 components, which I take to be Gaussian distributed with very wide width, i.e., with a uniform prior probability. In  $S/N$  space, the variance  $\mathcal{K}_{kk'}$  has off-diagonal terms affecting the largest scale  $S/N$  modes and complicating the interpretation of Fig. 1 for small  $k$ , but in the Bayesian analysis these unknowns can immediately be marginalized (by integrating over all  $c_k$ ).

Figure 1 also shows anomalies relative to the power-law theory at high  $k$  (see [5] for more examples). I model these residuals by an excess pixel noise with an amplification factor  $r$ . For FIRS,  $r \sim 0.25$ . For the two-year data, the most likely  $r < 1\%$  for the recommended DMR noise level for all maps, often zero for  $\nu_{\Delta T} > 0.2$  (and the results with  $r$  set to 0 differ very little). Features in Fig. 1 that do not fit the smooth theoretical model (around  $k \sim 200$  for  $53a + b$ ) represent unknown components, denoted by  $\text{res}_k$ , which could point to a better model power spectrum to try, or residuals left over from the various DMR map-processing techniques. In general, the  $\text{res}_k$  covariance  $\mathcal{R}$  would be nondiagonal. The nature of the low and high  $S/N$  modes has been probed with angular correlation functions [6]. These reveal the expected result that high  $S/N$  modes do indeed involve collective large scale pixel combinations, while low  $S/N$  modes involve destructive interferences from nearby pixels that are insensitive to large scale structure in the maps, but are quite sensitive to physics inside the beam, whether from systematic effects or true “white” noise on the sky. Thus  $S/N$  modes form an ideal set for filtering.

The first step in the Bayesian method is the construction of a joint likelihood function in  $\langle C_\ell \rangle_{\text{DMR}}^{1/2}$ ,  $\nu_{\Delta T}$ , and  $r$  (adopting a uniform prior probability in each). Integrating over  $r$  (marginalizing it) allows one to construct  $\nu_{\Delta T}$ - $\langle C_\ell \rangle_{\text{DMR}}^{1/2}$  contour maps. Marginalization over  $\nu_{\Delta T}$  or cuts along a given  $\nu_{\Delta T}$  (e.g., 0) gives a  $\langle C_\ell \rangle_{\text{DMR}}^{1/2}$  distribution; marginalization over  $\langle C_\ell \rangle_{\text{DMR}}^{1/2}$  gives a  $\nu_{\Delta T}$  distribution. Table I gives 50% Bayesian probability values for  $\langle C_\ell \rangle_{\text{DMR}}^{1/2}$  and  $\nu_{\Delta T}$ , with “one-sigma” error bars from the 84% and 16% Bayesian values, “two-sigma” from the 97.5% and 2.5% values. The  $\langle C_\ell \rangle_{\text{DMR}}^{1/2}$  for all of the 53, 90, and 31 GHz DMR maps and FIRS map agree at better than the one-sigma level, along fixed  $\nu_{\Delta T}$  lines, among different  $\nu_{\Delta T}$ , and when  $\nu_{\Delta T}$  is marginalized, essentially independently of the degree of  $S/N$  filtering (cuts at 200 are shown). There is also no discernable power in the DMR  $a - b$  maps. These band powers compare with the original first year DMR number, using correlation functions (CF) [1],  $0.97 \pm 0.28$ ; a later update [11],  $0.97 \pm 0.16$  using the Boughn-Cottingham single quadratic statistic (for  $\nu_{\Delta T} = 0$ ); the two-year data, using CF [2],  $1.06 \pm 0.09$  (for  $\nu_{\Delta T} = 0$ ) and  $1.03_{-0.31}^{+0.44}$  (for the most probable  $\nu_{\Delta T}$ ); and the FIRS ( $+q$ ) CF result [12],  $1.08 \pm 0.3$ .

The tilts shown in the table (with one- and two-sigma errors) are not determined with the same precision, nor can one attach the same confidence to the values, because

TABLE I. The second and third rows give band-powers (marginalized over  $\nu_{\Delta T}$ ) and power-spectrum slopes (marginalized over  $\langle C_\ell \rangle^{1/2}$ ) for the various DMR and FIRS maps listed in row 1 (some using just the top 200  $S/N$  modes). The fifth and sixth rows show that  $10^5 \langle C_\ell \rangle^{1/2}$  for fixed  $\nu_{\Delta T}$  derived for all the maps (listed in row 3) are compatible, and are insensitive to  $\nu_{\Delta T}$ .

$a + b$ ch	53 + 90 + 31	All(200)	53	53(200)	53,+ $q$	53,+ $q$ (200)	90	31	FIRS
$10^5 \langle C_\ell \rangle_{\text{DMR}}^{1/2}$	$1.12 \pm 0.13$	$1.13 \pm 0.13$	$1.08 \pm 0.12$	$1.16 \pm 0.16$	$1.03 \pm 0.10$	$1.08 \pm 0.12$	$1.16 \pm 0.15$	$0.96 \pm 0.27$	$1.23 \pm 0.27$
$\nu_{\Delta T} + 1$	$1.3_{-0.3;0.6}^{+0.3;0.6}$	$1.4_{-0.4;0.9}^{+0.4;0.8}$	$1.4_{-0.4;0.9}^{+0.4;0.7}$	$1.0_{-0.5;0.8}^{+0.5;0.9}$	$1.7_{-0.4;0.8}^{+0.3;0.6}$	$1.3_{-0.5;0.9}^{+0.5;0.9}$	$1.6_{-0.5;1.0}^{+0.5;0.9}$	$1.8_{-1.0;1.6}^{+0.8;1.1}$	$1.6_{-0.8;1.4}^{+0.7;1.2}$
Channel	53a	53b	53a - b	90a	90b	90a - b	31a	31b	FIRS
$(\nu_{\Delta T} = 0)$	$1.26 \pm 0.12$	$1.06 \pm 0.15$	$0.30_{-0.30}^{+0.22}$	$0.82 \pm 0.28$	$1.24 \pm 0.21$	$0_{-0}^{+0.29}$	$0.82 \pm 0.39$	$0.84 \pm 0.45$	$1.15 \pm 0.28$
$(\nu_{\Delta T} = 1)$	$1.13 \pm 0.11$	$0.97 \pm 0.12$	$0.36_{-0.25}^{+0.16}$	$0.91 \pm 0.26$	$1.22 \pm 0.17$	$0_{-0}^{+0.33}$	$0.86 \pm 0.39$	$0.91 \pm 0.47$	$1.28 \pm 0.25$

of the variation with filtering. In particular, the high point for the 53a + b  $S/N$  power in Fig. 1 just below  $k = 200$  (which comes from 53a and not from 53b) drives the index up somewhat, as do the two slightly high points around 100 (which 90a + b has also), while the low point at 70 drives it down. Thus the most probable index is sensitive to filtering, as Fig. 1 makes clear; it also shows a high index power law is *not* a particularly good description of the excess power. Another significant feature is that the low quadrupole drives the index higher (the “+ $q$ ” results). I do not actually have to subtract the quadrupole since the large uniform prior allows the analysis to attribute what it cannot fit to  $c_k$ . I agree with the DMR team [13] that the lower indices obtained by assuming Galactic interference in the quadrupole are the better numbers to adopt. Decreasing the beam size also lowers  $\nu_{\Delta T}$  a bit [6]. The  $\nu_{\Delta T}$  results compare with the original first year DMR value [1],  $1.2_{-0.7}^{+0.5}$ ; the two-year corrected CF result [2]  $1.1_{-0.4}^{+0.4}$  ( $1.4_{-0.4}^{+0.4}$  for + $q$ ); two-year power spectrum (PS) values using quadratic estimators [14],  $1.5_{-0.4}^{+0.4}$  (for  $3 \leq \ell \leq 19$ ),  $1.3_{-0.5}^{+0.4}$  (for  $3 \leq \ell \leq 30$ ), and using Bayesian methods with linear multipole filtering [13],  $0.96_{-0.4}^{+0.4}$ , (for  $3 \leq \ell \leq 30$ ) and for + $q$ ,  $1.2_{-0.3}^{+0.3}$ . The FIRS CF value [12] is  $1.0_{-0.5}^{+0.4}$  including the quadrupole, whereas I get  $1.8_{-0.8;1.5}^{+0.6;1.0}$  for FIRS, + $q$ , and  $\text{res}_k$  is large enough that direct  $S/N$  filtering can give even higher values [6].

I have found sharp  $S/N$  filtering preferable for statistical analysis [15], but smooth preferable for cleaning noise to look for robust map-independent features. Figure 1 shows optimally filtered maps and their temperature autocorrelation functions,  $C(\theta)$ . The maps are equal area projections [16] about the pole. Floating averages, dipoles, and quadrupoles can be added to bring them into better agreement. This Wiener filtering is an immediate byproduct of the  $S/N$  eigenmode expansion [5,17]; given observations  $\bar{\xi}_k$ , the mean value and variance matrix of the desired signal  $s_k$  are

$$\langle s_k | \bar{\xi} \rangle = \sum_{k'} \{ \mathcal{E}_{TR} \mathcal{E}_{\text{tot}R}^{-1} \}_{kk'} \bar{\xi}_{k'},$$

$$\langle \Delta s_k \Delta s_{k'} | \bar{\xi} \rangle = \{ \mathcal{E}_{TR} \mathcal{E}_{\text{tot}R}^{-1} (\mathcal{E}_{\text{tot}R} - \mathcal{E}_{TR}) \}_{kk'}.$$

The mean field  $\langle s_k | \bar{\xi} \rangle$  is the maximum entropy solution. The operator multiplying  $\bar{\xi}_k$  is the Wiener filter. The fluctuation,  $\Delta s_k = s_k - \langle s_k | \bar{\xi} \rangle$ , of the signal about the mean is realized by multiplying a vector of  $N_{\text{pix}}$  independent Gaussian random numbers by the square root of the variance matrix.

The Wiener filter depends upon the  $\langle C_\ell \rangle_{\text{DMR}}$  and  $\nu_{\Delta T}$  we choose; I use the maximum likelihood value for  $\langle C_\ell \rangle_{\text{DMR}}$ , and both maps and correlation functions are relatively insensitive to  $\nu_{\Delta T}$  for large scale features. When the noise is large, as it is for these maps, it is the higher  $\ell$  power that is preferentially removed by optimal filtering. Thus the theoretical fluctuation  $\Delta s_k$  would have to be added to the Wiener-filtered maps of Fig. 2 to give a realistic picture of the sky given the data and the theory. That is, the maps are too smooth, 31 GHz the most, 53 GHz the least. The optimally filtered correlation functions for *both* 53 and 90 GHz converge to the raw 53 GHz correlation function, and are  $\nu_{\Delta T}$  independent (but this does not address how statistically significant such a  $C(\theta)$  is for the given  $\nu_{\Delta T}$ ). Not shown are the  $C(\theta)$  for the optimally filtered DMR  $a - b$  difference maps, but these are nicely zero. Also not shown, but very gratifying, is that the main features are evident in both  $A$  and  $B$  channel maps, including in the noisy 90a and 31a,b.

Thus with  $S/N$  modes one can analyze the full map, identify residual problems in the maps, and easily explore the statistical robustness to varying levels of  $S/N$  filtering. This Letter shows that the overall anisotropy power COBE has discovered exists in all channels and is very robust. The index is compatible with inflation values within the errors for all maps; and in those maps with high mean  $\nu_{\Delta T}$ , what drives it up is more indicative of leftover residuals than high-tilt primary anisotropies. The method also gives the most sensitive errors on band power as a function of  $\nu_{\Delta T}$ : for 53a + b,  $10^5 \langle C_\ell \rangle_{\text{DMR}}^{1/2} \approx [0.98 + 0.18(1 - \nu_{\Delta T}/2)^{2.5}] \times 1_{-0.1}^{+0.09}$ ; and for (53 + 90 + 31)a + b,  $\approx [0.93 + 0.28(1 - \nu_{\Delta T}/2)^{2.5}] \times 1_{-0.07}^{+0.08}$ . These formulas can be used to normalize inflation-based models of cosmic structure formation which are then strongly constrained by cluster abundance observations [18].

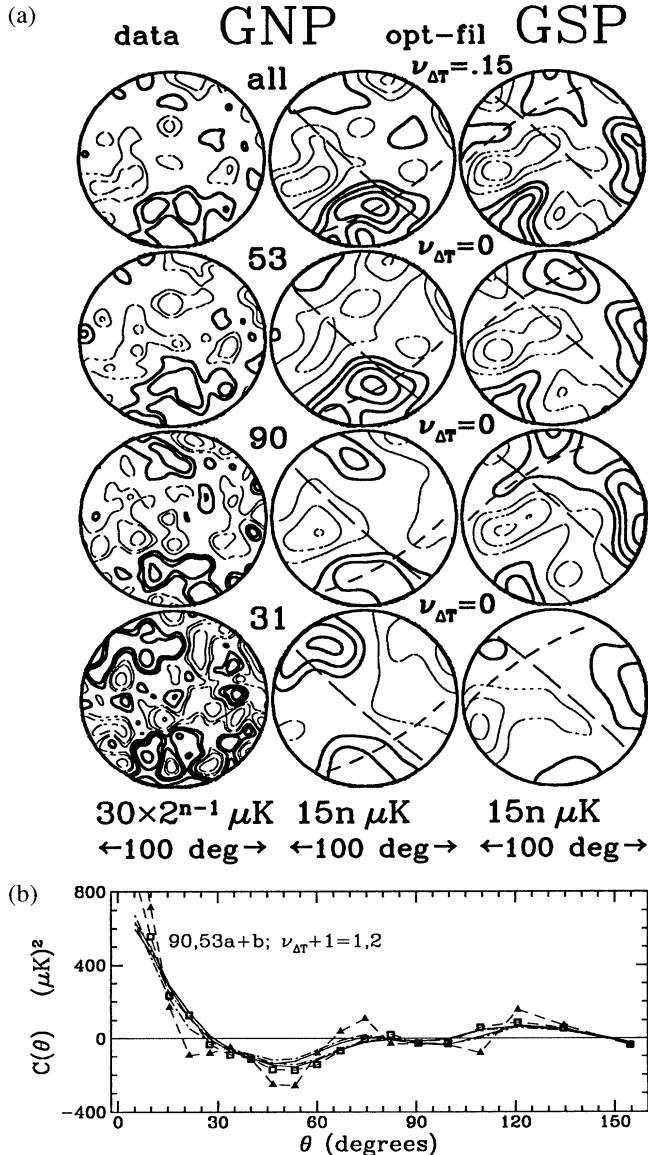


FIG. 2. In the upper figure, the first column shows unfiltered 100° diameter DMR  $a + b$  maps centered on the North Galactic Pole, the second shows them after Wiener filtering, the third the South Pole version, with the  $n$ th contour as noted and negative contours heavier than positive ones. The maps are only weakly dependent upon the  $\nu_{\Delta T}$  choice: the 53 + 90 + 31 map uses 0.15, the rest 0. The  $x$  axis points to the Galactic center, the  $y$  axis to  $\hat{q}_{GNP} \times \hat{q}_{GC}$ , the supergalactic plane is long dashed, and the ecliptic plane is short dashed; all are uncorrelated with the features. The maps have been smoothed by a 3° Gaussian filter. In the lower figure, correlation functions for 53a + b GHz (open circles) and 90a + b GHz (solid triangles) are contrasted with  $\nu_{\Delta T} = 0, 1$  Wiener-filtered  $C(\theta)$ 's for both cases; all but the unfiltered 90a + b GHz one agree, and it does within its errors.

This research was supported by NSERC and the Canadian Institute for Advanced Research.

[1] G.F. Smoot *et al.*, *Astrophys. J. Lett.* **396**, 1 (1992).  
 [2] C. Bennett *et al.*, *Astrophys. J.* **436**, 423 (1994).  
 [3] K. Ganga *et al.*, *Astrophys. J. Lett.* **410**, 57 (1993).  
 [4] J.R. Bond, in *Proceedings of the IUCAA Dedication Ceremonies, Pune, India, 1992*, edited by T. Padmanabhan (Wiley, New York, 1994).  
 [5] J.R. Bond, *Astrophys. Lett. Comm.* (to be published).  
 [6] J.R. Bond, in *Proceedings of the 8th Nishinomiya-Yukawa Memorial Symposium*, edited by M. Sasaki (Academic Press, New York, 1994).  
 [7] J.R. Bond and G. Efstathiou, *Mon. Not. R. Astron. Soc.* **226**, 655 (1987).  
 [8] J.R. Bond, J.R. Crittenden, R.L. Davis, G. Efstathiou, and P.J. Steinhardt, *Phys. Rev. Lett.* **72**, 13 (1994).  
 [9] R. Kneissl and G. Smoot, COBE Note 5053 (1993).  
 [10] C. Lineweaver and G. Smoot, COBE Note 5051 (1993).  
 [11] E.L. Wright *et al.*, *Astrophys. J.* **420**, 1 (1994).  
 [12] K. Ganga, L. Page, E. Cheng, and S. Meyer, *Astrophys. J. Lett.* **432**, 15 (1994).  
 [13] K. Gorski *et al.*, *Astrophys. J. Lett.* **430**, 89 (1994).  
 [14] E.L. Wright *et al.*, *Astrophys. J.* **436**, 443 (1994).  
 [15] Filtering using  $S/N$  modes has a long history in signal processing where it is called the Karhunen-Loeve method. Smooth measures (e.g.,  $\propto \mathcal{E}_{TR,k}$  or Wiener based) can be effective for estimation of  $\langle C_\ell \rangle$  but not  $\nu_{\Delta T}$ ; e.g.,  $\propto \sum \mathcal{E}_{TR,k} \xi_h^2$  which includes the constraints in a single optimally weighted quadratic estimator of  $\langle C_\ell \rangle$ , which yields band powers compatible with those in Table I.  
 [16] The coordinates [7] are  $2 \sin(\theta/2) (\cos \phi, \sin \phi)$ .  
 [17] E.F. Bunn *et al.*, *Astrophys. J. Lett.* **432**, 75 (1994), have independently applied Wiener filtering, to the “reduced galaxy” first-year DMR map, a linear combination of the three frequency maps, using rather different methods.  
 [18] Using a formula in [6,19] relating  $\sigma_8$  — the rms linear density fluctuations on cluster scales ( $8h^{-1}$  Mpc, where  $h$  is Hubble’s constant in units of  $100 \text{ km s}^{-1} \text{ Mpc}^{-1}$ ) — which was used to normalize models before COBE to  $\langle C_\ell \rangle_{\text{DMR}}^{1/2}$ , for  $\Omega = 1$  tilted cold dark matter models we have  $\sigma_8 \approx 1.36 e^{2.63\nu_s} [2\nu_s e^{-2\Omega_B} - 0.06] / [0.85(1 + \tilde{r}_{is})^{1/2}] [1 + 0.2\{(1 - 0.54\nu_s)^{2.5} - 1\}]$  — for the (53 + 90 + 31)a + b map. Here  $\Omega_B$  is the fraction of mass in baryons,  $\nu_s = n_s - 1$  is the initial tilt for adiabatic scalar fluctuations, and the ratio of gravity-wave-induced to scalar-induced contributions to the DMR band power is  $\tilde{r}_{is}$  — which is  $\approx -6\nu_t$ , where  $\nu_t$  is the tilt in the gravity wave spectrum. Often  $\nu_t \approx \nu_s$ , but for some inflation models  $\nu_t \approx 0$ , hence  $\tilde{r}_{is} \approx 0$  [6,8,19]. If there is one species of light neutrino of mass density  $\Omega_\nu < 0.3$  in addition to the cold dark matter of density  $1 - \Omega_\nu - \Omega_B$ , the formula should be further multiplied by  $[1 + 0.55(\Omega_\nu/0.3)^{1/2}]^{-1}$ . X-ray cluster observations favor  $\sigma_8 \sim 0.6 - 0.7$  for  $\Omega = 1$  (e.g., [19]), which gives  $n_s > 0.7$  if  $\nu_t = 0$  and  $n_s > 0.82$  if  $\nu_t = \nu_s$ .  
 [19] J.R. Bond, in *Theory and Observations of the Cosmic Background Radiation*, Proceedings of the Les Houches Summer School, Session LX, edited by R. Schaeffer (Elsevier, New York, 1995).